

## Oxidation of membrane curvature-regulating phosphatidylethanolamine lipid results in formation of bilayer and cubic structures

*Shalene Sankhagowit,<sup>a</sup> Ernest Y. Lee,<sup>b</sup> Gerard C. L. Wong,<sup>b</sup> and Noah Malmstadt<sup>a\*</sup>*

<sup>a</sup>Mork Family Department of Chemical Engineering and Materials Science,  
University of Southern California, Los Angeles, CA 90089, USA

<sup>b</sup>Bioengineering Department, Chemistry & Biochemistry Department, California Nano Systems Institute, University of California, Los Angeles, CA 90095, USA

### SUPPLEMENTARY INFORMATION

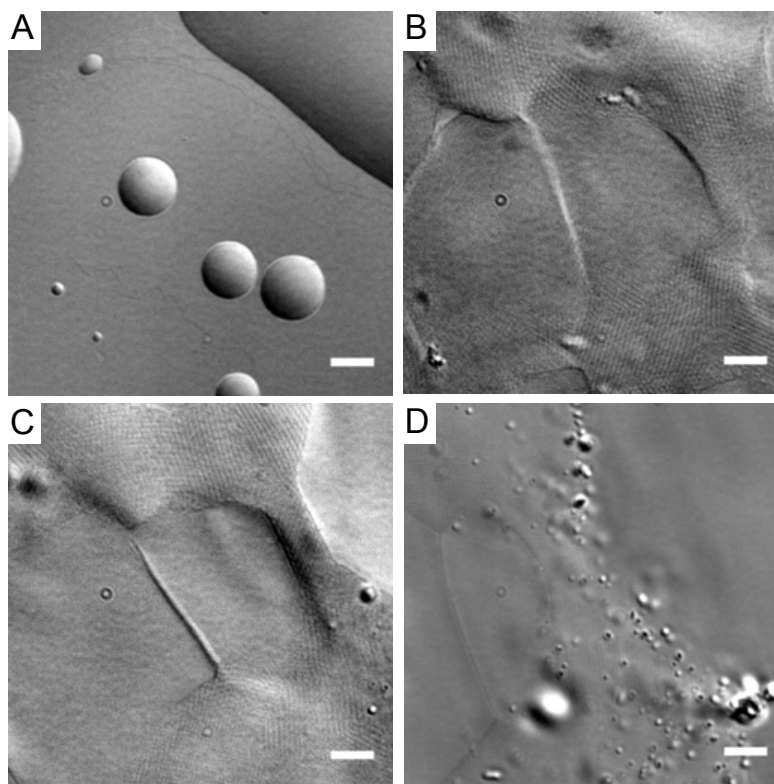


**Figure S1.** Hydration of 24-hour oxidized DOPE lipid (high magnification). (A) Dried lipid film and hydrated film at (B) 10, (C) 45, and (D) 60 min after addition of water. Scale bars = 5  $\mu\text{m}$ .

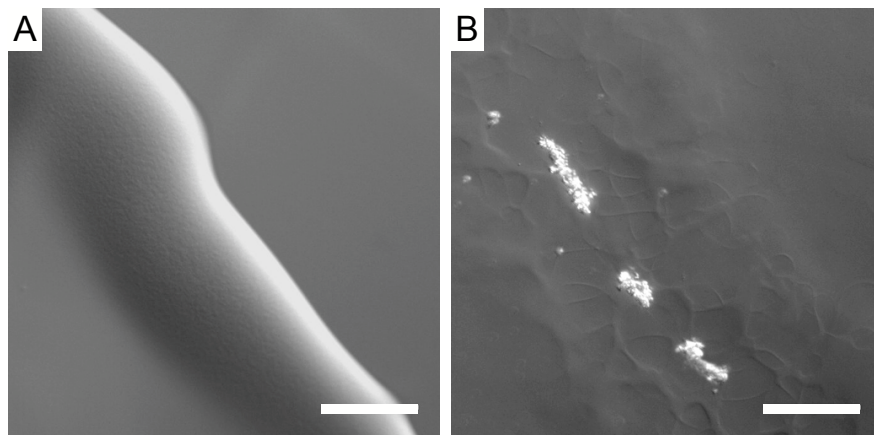


**Figure S2.** Hydrated oxidized DOPE lipid (low magnification). (A) Dried lipid film and (B) hydrated lipid film 5 min after addition of water. Scale bars = 50  $\mu\text{m}$ .

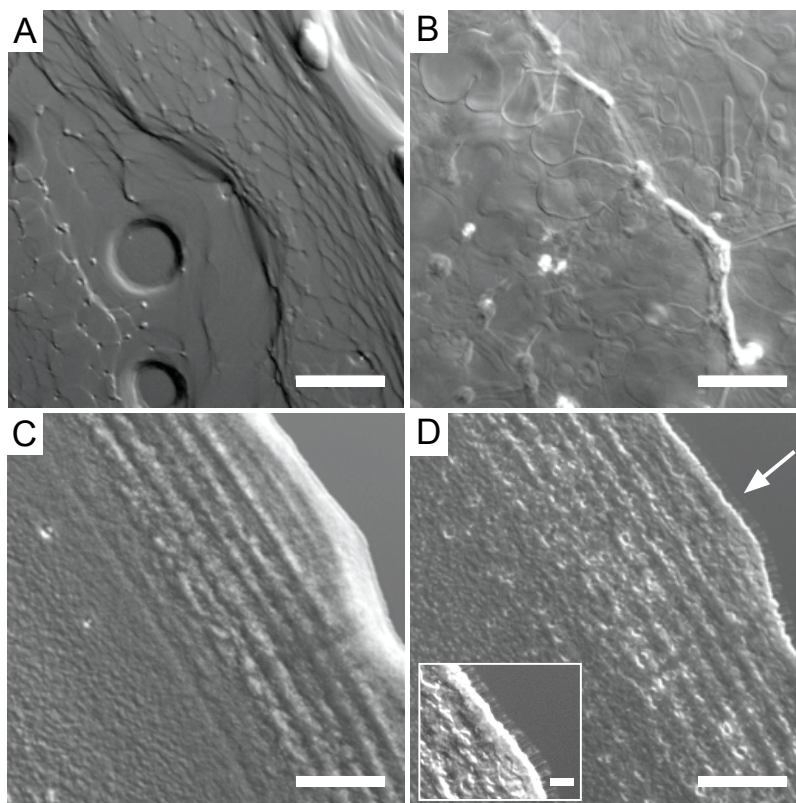


**Figure S3.** Comparison of lamellar and non-lamellar phases in water (low magnification). DOPC (lamellar phase): (A) dried and (B) 5 min after hydration. DOPE (inverted hexagonal phase at room temperature): (C) dried and (D) 5 min after hydration. Note that a small fraction of DOPE was oxidized due to air exposure and formed tubules along the lipid film edge (arrow and inset). Scale bars = 50  $\mu\text{m}$  (10  $\mu\text{m}$  for inset).

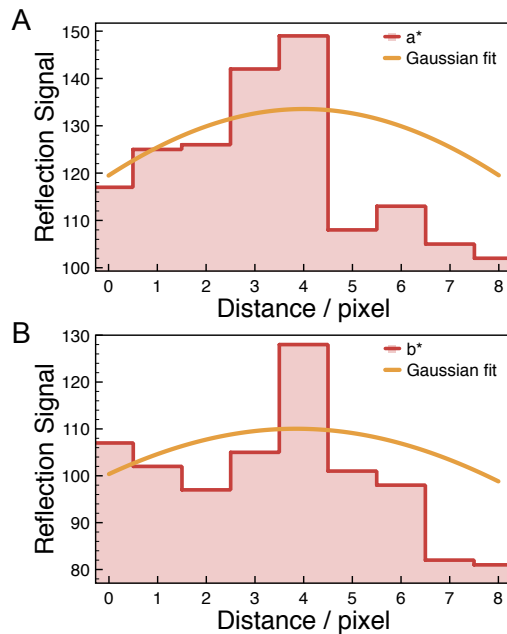


**Figure S4.** (Red) Profiles of the reflection signal corresponding to reciprocal lattice vectors (A)  $a^*$  and (B)  $b^*$  and (yellow) their corresponding fitted Gaussian functions.

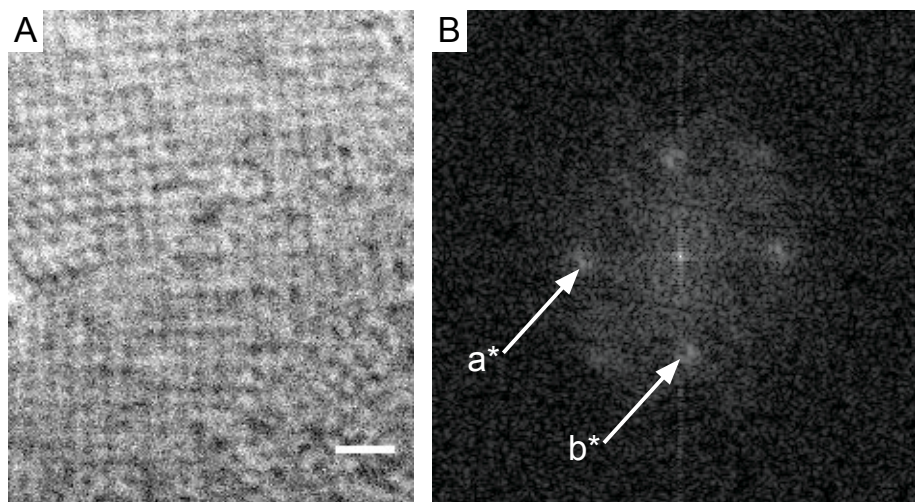


**Figure S5.** (A) Section from Figure 1C showing the magnified lattice structure of oxidized DOPE. Scale bar =  $2 \mu\text{m}$ . (B) Two-dimensional fast Fourier transform of (A); the indicated reflections correspond to reciprocal lattice vectors  $a^*$  and  $b^*$ . The angle between the reflections is approximately  $92^\circ$ , and the lattice parameters are  $a = 304 \text{ nm}$  and  $b = 309 \text{ nm}$ .

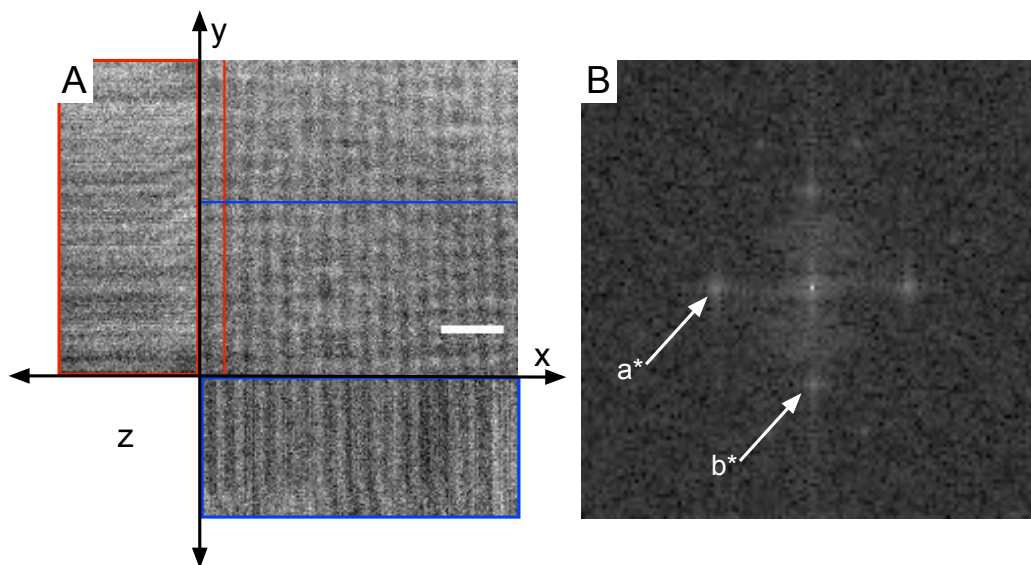


**Figure S6.** (A) Cross sections of a three-dimensional image stack of the lattice structure of hydrated oxidized DOPE, spanning  $10.1 \mu\text{m} \times 10.1 \mu\text{m} \times 4.42 \mu\text{m}$  (x-y-z). Scale bar =  $2 \mu\text{m}$ . (B) Two-dimensional fast Fourier transforms at an x-y cross-section; the indicated reflections correspond to reciprocal lattice vectors  $a^*$  and  $b^*$ . The angle between reflections is  $90^\circ$ , and the lattice parameters are  $a = b = 574 \text{ nm}$ .

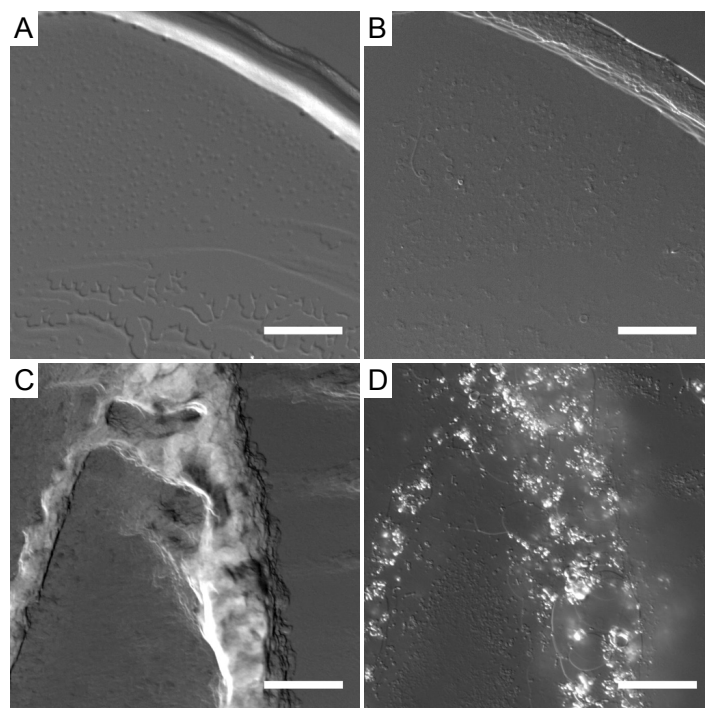


**Figure S7.** Lipid films of DOPE/lyso-PE mixtures showing lamellar phase structures (low magnification). (A) Dried and (B) 5 min after hydration of 60 mol% DOPE/40 mol% lyso-PE and (C) dried and (D) 5 min after hydration of 5 mol% DOPE/95 mol% lyso-PE. Scale bars =  $50 \mu\text{m}$ .

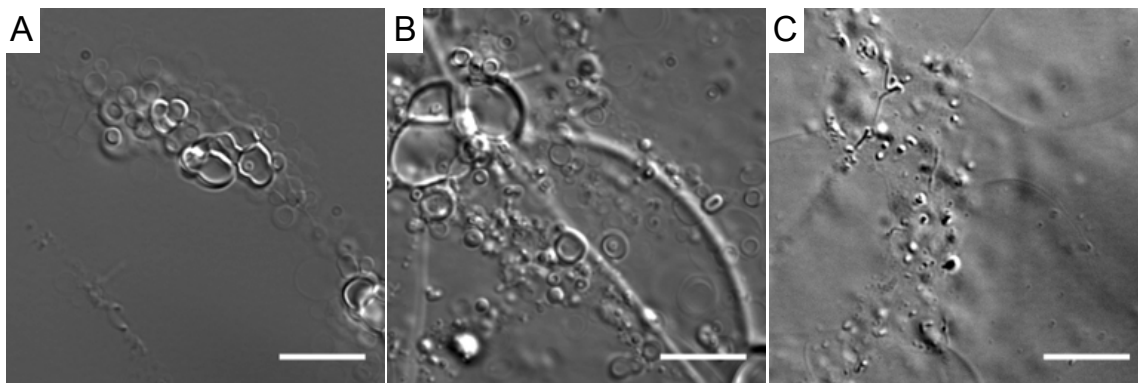


**Figure S8.** Hydrated lipid films of (A) 60 mol% DOPE/40 mol% lyso-PE, (B) 5 mol% DOPE/95 mol% lyso-PE, and (C) oxidized DOPE dried at the same lipid concentration (approximately 0.7 mg/mL), 5 min after addition of water. Scale bars = 10  $\mu$ m.

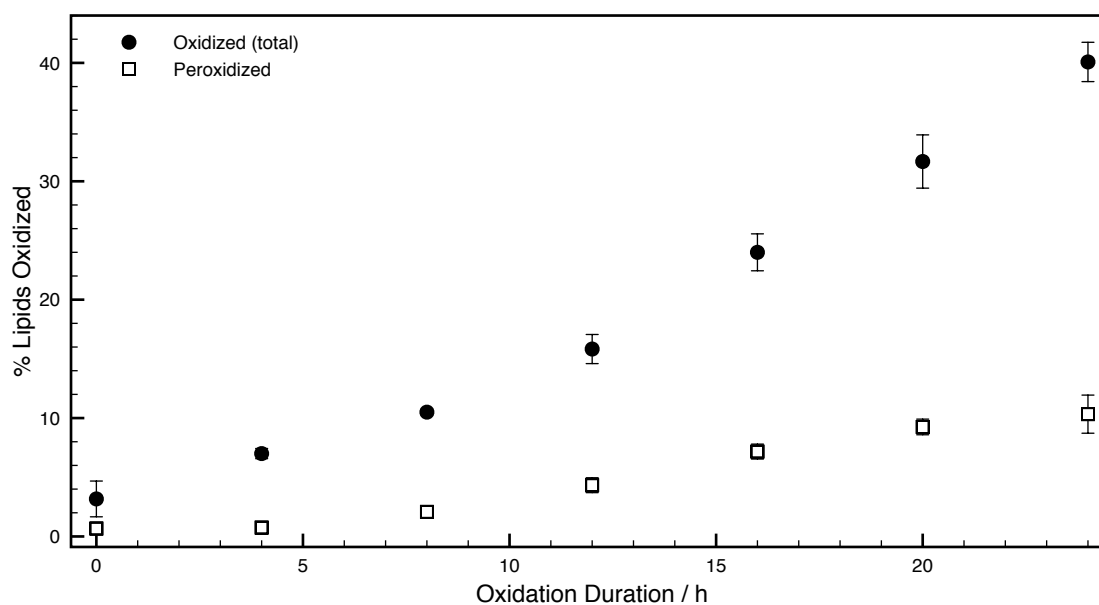


**Figure S9.** Relative amounts of total oxidized (filled circles) and peroxidized (open squares) DOPE with duration of oxidation. The total oxidized amount was estimated as deductions by the amount of vinyl protons present (i.e. this data is complementary to Figure 5c); the amount of peroxidized lipid was estimated by integrating the shifted vinyl peak shown in Figure 5b, again with respect to the glycerol proton peak.

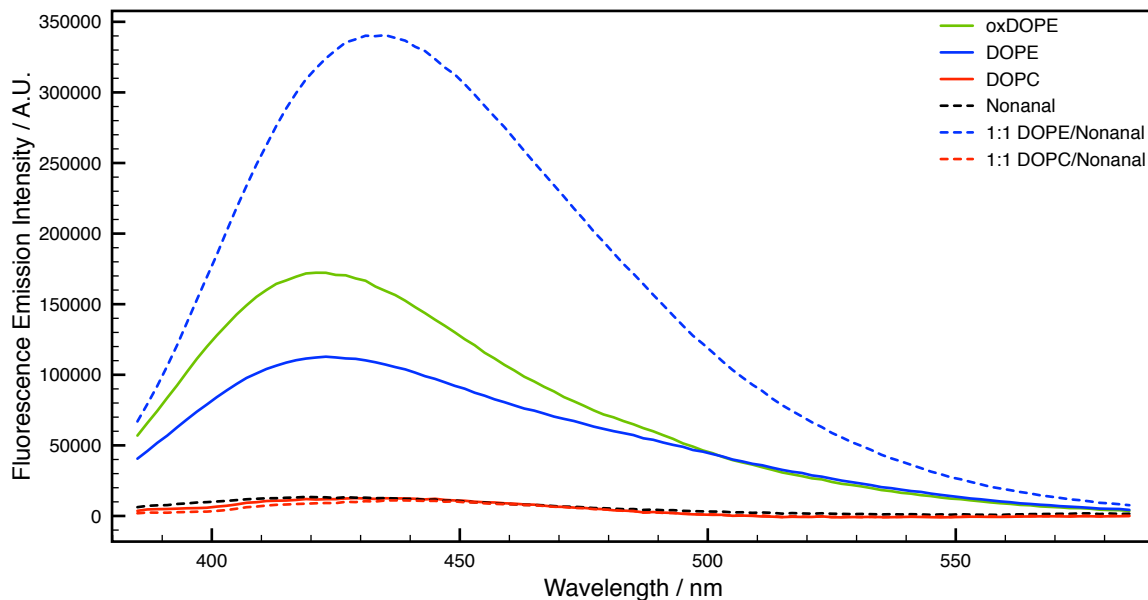


**Figure S10.** Fluorescence emission of DOPE and DOPC samples for detection of Schiff base formation.

As briefly discussed in the main text, the amine group of the PE lipid head group can participate in a condensation reaction with the aldehyde group, formed through lipid tail scission during oxidation, to form fluorescent Schiff base products. Here, lipid samples in chloroform were excited at 365 nm and their emissions were measured at 385-585 nm (QuantaMaster 4 Spectrofluorometer, PTI). All samples were stored overnight under vacuum as dried lipid films and were then dissolved in chloroform to 5 mg/mL on the following day. The oxidized DOPE sample (oxDOPE) was prepared by subjecting the dried sample to an air stream for 4 hours before overnight storage under vacuum. Nonanal (Sigma-Aldrich) was used to mimic tail scission fragments and was added to DOPE and DOPC samples in 1:1 molar ratio of lipid-to-nonanal before the drying step. Figure S10 shows that none of the DOPC-containing samples emitted fluorescence with excitation at 365 nm. All DOPE samples (control, oxDOPE, and with nonanal) were fluorescent, possibly due to some unintended oxidation. Note that the nonanal-containing sample exhibited the highest fluorescence emission intensity that corresponds to the highest amount of Schiff base products formed.